PRAMANA — journal of physics

Vol. 77, No. 5
November 2011
pp. 975–986

Linearity stabilizes discrete breathers

T R KRISHNA MOHAN[1,*] and SURAJIT SEN[2]

[1]CSIR Centre for Mathematical Modelling and Computer Simulation (C-MMACS), NAL Wind Tunnel Road, Bangalore 560 037, India
[2]Department of Physics, State University of New York, Buffalo, New York 14260-1500, USA
*Corresponding author. E-mail: kmohan@cmmacs.ernet.in

Abstract. The study of the dynamics of 1D chains with both harmonic and nonlinear interactions, as in the Fermi–Pasta–Ulam (FPU) and related problems, has played a central role in efforts to identify the broad consequences of nonlinearity in these systems. Here we study the dynamics of highly localized excitations, or discrete breathers, which are known to be initiated by the quasistatic stretching of bonds between adjacent particles. We show via dynamical simulations that acoustic waves introduced by the harmonic term stabilize the discrete breather by suppressing the breather's tendency to delocalize and disperse. We conclude that the harmonic term, and hence acoustic waves, are essential for the existence of localized breathers in these systems.

Keywords. Intrinsic localized modes; discrete breathers; acoustic vacuum; Fermi–Pasta–Ulam systems; breather stability.

PACS Nos 63.20.Pw; 63.20.Ry

1. Introduction

Fermi, Pasta and Ulam's computational study of particle dynamics in a 1D system of masses connected via nonlinear springs [1] ushered a new era in the study of nonlinear many-particle systems [2,3]. We consider Hamiltonians of the following general form:

$$H = \sum_{i=1}^{N} \frac{p_i^2}{2m_i} + \sum_{i=1}^{N} V\left(|x_{i+1} - x_i|\right), \tag{1}$$

where we set $m_i \equiv m$ and let x_i refer to the displacement of particle i from its equilibrium position. N is the number of particles in the system. We now set

$$V\left(|x_{i+1} - x_i|\right) \equiv \frac{\alpha}{2}\left(x_{i+1} - x_i\right)^2 + \frac{\beta}{n}\left(x_{i+1} - x_i\right)^n, \tag{2}$$

where n is here taken to be an even number >2 [4–14].

Our focus here will be on the interplay of the harmonic and nonlinear terms in eq. (2). To start with, we look at the purely nonlinear case, i.e. when $\alpha = 0$. Due to the absence of the harmonic term in eq. (2), no acoustic propagation is allowed in the system,

DOI: 10.1007/s12043-011-0200-6; ***e*Publication: 26 October 2011**

i.e., sustained particle oscillations about the original equilibrium position of any particle becomes inadmissible. In the context of Hertz systems, Nesterenko [15–18] and others [19–29] have shown that these systems, being intrinsically nonlinear, quite often exhibit dynamical properties different from those systems where acoustic oscillations are allowed. Much theoretical, simulational and experimental work has been done in the context of unloaded, discrete granular systems in acoustic vacua [22–30]. In 1D, these systems admit solitary waves, allow the formation of secondary solitary waves when solitary waves collide [31–34] and exhibit the recently suggested quasiequilibrium phase in finite systems [35–38].

We note that analytical work on the dynamics of the purely nonlinear regime is quite difficult and comprehensive analysis practically inachievable at the present time. Nevertheless, significant results have been obtained analytically and the existence of 'discrete breathers' (DBs) (see below) in such systems established (see §4.1.3 in Flach and Gorbach [39] and references therein for an overview of the analytic results). Accurate dynamical simulations are nevertheless essential to help in the development of physical insights into this regime. In this context we note that several groups have made significant contributions to the area [10,39–44]. The present computational study reports the dynamical consequences of the presence of α in eq. (2) in the context of stability of DBs.

Dynamics of purely nonlinear systems are usually highly sensitive to the initial and boundary conditions. In an earlier study, we have reported about the dynamics of systems described by eq. (2) when perturbed by a δ-function velocity perturbation imparted to any particle at an initial time $t = 0$ [36]. Velocity perturbations lead to very different system dynamics compared to that seen when the dynamics is initiated by displacement perturbations (see below). We explored the system dynamics for both periodic boundary conditions and fixed boundary conditions [36]. In the former case, $v_1 = v_{N+1}$ while, in the latter case, the particle velocities were simply reversed during collisions with a boundary. We reported about the calculations for cases with $\alpha = 0, \beta = 1$ (purely nonlinear), $\alpha = 1, \beta = 0$ (purely linear) and $\alpha = 1, \beta = 1$ (both linear and nonlinear effects of comparable strength) in eq. (2). When $\alpha = 0, \beta = 1$, such a perturbation results in both a stable propagating compression pulse (solitary wave), and an identical and opposite propagating dilation pulse (anti-solitary wave). The solitary and anti-solitary waves interact among themselves and with the boundaries leading to the eventual formation of an equilibrium-like state with excitations made up of a Gaussian energy distributed collection of only solitary and anti-solitary waves and hence with sustained large energy fluctuations [35–37]. In all our studies with $\alpha = 1$ and $\beta = 0, 1$, the system eventually slipped into a state where energy is equipartitioned. Such an eventual state would be expected for a harmonic oscillator chain. Interestingly, the solitary waves are comparatively more unstable in the presence of acoustic waves, which is in complete contrast with the DBs which stabilize further when $0 < \alpha \leq 1$.

Here we shall consider the system dynamics when, instead of a δ-function velocity perturbation at $t = 0$, one or more quasistatically displaced particles (displacement perturbation) are allowed to time-evolve with the system starting from rest. For $\alpha = 1, \beta = 0$, the bond vibrations efficiently disperse throughout the system. For $\alpha = 0, \beta = 1$, the bond vibration(s) can be identified as DBs and are localized and sustained across many decades in time with the system eventually beginning to slip into an equilibrium-like state with the qualification that the excitations in this state are comprised of solitary and

anti-solitary waves (as opposed to harmonic modes). We have referred to this kind of state which may show unusually large kinetic energy (and hence temperature) fluctuations, as the quasiequilibrium state [19,26,34–38].

Dynamics of the system when $\alpha = 1, \beta = 1$ is a well-studied problem [1,5,6,13,34–38]. Discrete DBs are very stable in this case and many experimental systems have been explored where these fascinating entities are being studied as, for example, in Bose–Einstein condensates, optical waveguides, molecular crystals, quasi-unidirectional solids, Josephson-junction arrays, layered silicates, micromechanical cantilever arrays, uranium crystals, pendulum arrays, shallow water, optical fibres, antiferromagnetic materials, photonic crystals and so on and so forth (see, for example, the reviews [13,41]). They are also expected to play a role in protein folding, defect migration, denaturation transitions and bubble formation in DNA etc. [13,41].

Here we focus on the stability aspect of DBs. In particular, we are interested to know what role the linearity plays in the stabilization of these entities. For this purpose, we treat linearity as a perturbation on the system in acoustic vacuum, i.e. the purely nonlinear system with $\alpha = 0, \beta = 1$. We increase the linearity in increments, holding $\beta = 1$, up to $\alpha = 1$ and investigate the increasing stabilization. We also observe the quasiequilibrium state as it changes to the pure equilibrium state of $\alpha = 1, \beta = 0$.

We conclude by noting the differences of the displacement perturbation systems from the velocity perturbation systems as the coefficient ratio between linearity and nonlinearity changes.

2. Details of computations

We solve the following coupled equations of motion for each of the particles in our system:

$$m\frac{\mathrm{d}^2x_i}{\mathrm{d}t^2} = -\alpha\left[(x_{i+1}-x_i)-(x_i-x_{i-1})\right] - \beta\left[(x_{i+1}-x_i)^{(n-1)}-(x_i-x_{i-1})^{(n-1)}\right]. \quad (3)$$

We set $m = 1$, $n = 4$ and $N = 100$ for most of the studies. In some cases, $N = 1000$ was also employed to confirm some aspects of the simulation. No new insights were obtained to warrant working with such large systems. Since enlarging the system does not yield any special insights and is computationally challenging, we contend that such large system calculations at this stage are not warranted. We have also carried out studies with $n = 6$ and 8. For steeper potentials, the challenge to maintain high accuracy in the integration of the equations of motion becomes formidable. Preliminary results lead us to expect that the findings reported here for the $n = 4$ case are broadly valid for larger even values of n.

We use the velocity-Verlet integration algorithm for carrying out the dynamical calculations [45]. The integration time step used was $\Delta t = 10^{-5}$. The integrations were typically run for 10^5 time steps. Energy conservation was accurate to 10 decimal places in our studies. We studied all the cases for both periodic and fixed boundary conditions. For fixed boundary condition studies, the masses of the particles at the edges were set to be infinitely large, thereby allowing reflection of any propagating energy from the fixed boundaries (this is the same as what was reported in ref. [36]). For periodic boundary conditions, we

imposed the condition that $x_{N+1} = x_1$ and $v_{N+1} = v_1$. As we shall see, the initial and the boundary conditions strongly influence the dynamics of these nonlinear systems, often leading to unexpected consequences.

To start off the integration, either velocity perturbation or displacement perturbation was employed. In the former case, the velocity of a single particle or a selected few, as the study warranted, was set different from zero, keeping others at rest. For displacement perturbation, two different scenarios exist. If a single particle is displaced away from its mean position and released from rest at the start of integration, odd-parity DBs result (see below). On the other hand, if two adjacent particles are displaced away from each other and released from rest at the start of integration, an even-parity DB results (see below).

3. Results

We have performed extensive dynamical simulations to probe the time-dependent behaviour of the coupled Newton's equations in eq. (3) for different values of α and β. Our emphasis has been on treating the linear term as a perturbation to the nonlinear term. Hence, we start by considering the purely nonlinear system with $\alpha = 0$ and $\beta = 1$. Then, we increase the linearity in steps by considering $\alpha = 10^{-4}, 10^{-3}, 10^{-2}, 10^{-1}$ and finally, $\alpha = 1$. We conclude subsequently by comparing the purely linear system with $\alpha = 1, \beta = 0$.

The results of our studies can be presented in a variety of ways and, indeed in a previous publication [36], some details such as the confirmation of the Gaussian distribution of velocities at late times (an expected result based on the Central Limit Theorem) and the existence of sustained large fluctuations in the average kinetic energy per particle has been discussed [19,35–38]. Also, in another publication [46], we discussed how the potential energy imparted for an even-parity perturbation (where two particles are perturbed initially) or in an odd-parity perturbation (where one particle has been initially perturbed) gradually gets dispersed into the system. Both of these cases lead to the emergence of long-lived localized excitations – the so-called DBs. Our studies suggest that an appropriate way of studying this energy dispersion process may be via contour plots with the magnitude of energy plotted against particle position and time (energy–density plots). We shall follow the same approach here and present the energy–density plots for different cases. But, first, here is a summary of the results we obtained in our earlier study (see, for details, [46]).

A displacement perturbation initially stores all energy as potential energy and hence in the perturbed bonds that connect these particles at time $t = 0$. The dynamics that follows has two essential features: (i) the bond energies must delocalize and (ii) average kinetic and potential energies must be $2E/3N$ and $E/3N$ respectively for the purely nonlinear case. In [46], we presented arguments to substantiate these two conditions. It is easy to see that the Poisson bracket of $L(t) = \sum_j x_{j+1}(t) - x_j(t)$, a time-dependent collection of bond lengths, with the Hamiltonian of eq. (1) does not commute and, therefore, $L(t)$ is not a constant of the motion. This tells us that the bond energies must delocalize. Virial theorem gives us that average kinetic energy is $2E/3N$ and average potential energy is $E/3N$, for the purely nonlinear case; both (average) kinetic and potential energies are $E/2N$ for the purely linear system. However, the re-distribution of energies into the above asymptotic values is a slow process in the purely nonlinear case because, in the purely nonlinear system, no acoustic

waves are possible and only solitary and anti-solitary waves can exist. Solitary waves have a specified width (dependent on n of eq. (2); see, for example, [19]) and, bundling energy into such a rigorously defined entity is a slow and painful process. As such, the leakage of energy from the DBs is slow and the equilibrium like state is attained very slowly allowing the DBs to survive for long.

The odd-parity and even-parity breathers behave differently. The former is less stable than the latter. The former also splits into three branches at early times; the two lateral branches are equidistant from the central one. The boundary conditions play an important role. In the case of periodic boundary conditions, the breather has only to contend with the collisions from the solitary waves that go around the chain after leaking out from the breather. This allows the breather to be more stable in the periodic boundary case than in the fixed boundary case. In the case of the latter, the solitary waves released from the breather through energy leakage bounce off the boundary walls and return to collide with the breather at various time depending on the distance to the walls. If the breather is not equidistant from the walls, this can cause unequal pressures which force the breather to be pushed laterally away from the closest wall. To summarize, maximum disturbance to the breather occurs, in general, in the fixed boundary case.

Introduction of acoustic waves by turning on the linear term by setting $\alpha \neq 0$ brings in significant changes and, quite counterintuitively, the breathers get stabilized further. In reality, we know that [9,13] the breather mode exists outside the acoustic spectrum and is incommensurate with it; typically, the acoustic spectrum has cut-off frequencies limiting its bandwidth. This prevents the coupling of the breather mode with the acoustic spectrum and hence no energy leakage is possible into the acoustic waves. But, solitary waves still exist because of the presence of nonlinear term and the leakage into it continues, albeit in a much reduced manner because of the instability of the solitary waves in the presence of the acoustic waves [35–37].

We now present the results of the perturbation study. In figure 1, we present the results for the odd-parity breather in the fixed boundary case. In figure 1a, we see the purely nonlinear case and, as already discussed, the breather splits characteristically into three branches. One can also see that the breather is pushed away fom the nearest wall by the solitary waves bouncing off it. $\alpha = 10^{-2}$ in figure 1b and we can already see that breather survives longer even though it is being rattled much by the solitary waves bouncing back from the boundaries. Note that the solitary waves are marked by the radiating lines of constant grey levels in the figure. In figure 1c, we find that the breather has become much more stable even though it is moving around much. Figure 1d is the common situation found in the literature where $\alpha = 1$, $\beta = 1$. We note here that the odd-parity breather does not keep its position unlike the even-parity breather (see later; see also figures 4 and 5) and moves from one boundary to the other in the fixed boundary case (see also [46]). Furthermore, the typical appearance of the odd-parity breather in the purely nonlinear case, with its three branches, is missing in this situation where α is comparable in strength with β. Nevertheless, if one examines the particle dynamics closely, as in the instantaneous velocity profile of the chain of figure 2, we see that the particle dynamics remains different in the odd- and even-parity cases and it is only the appearance in the energy–density plots that has become similar. This is under further investigation.

The differences that result when the boundary condition is changed to that of periodic boundary is seen in figure 3. We see that the breather holds its position and does not move

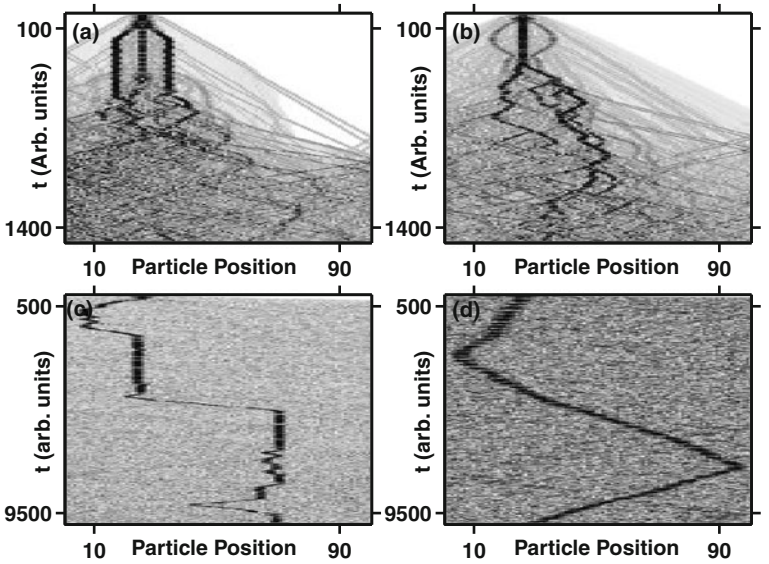

Figure 1. Odd-parity breather (initiated by a single-particle displacement perturbation) between fixed boundaries for different values of α, with $\beta = 1$ of eq. (2). For (**a**) $\alpha = 0$, (**b**) $\alpha = 10^{-2}$, (**c**) $\alpha = 10^{-1}$ and (**d**) $\alpha = 1$. It is seen that the breather stabilizes better as α increases.

around as in the fixed boundary case (figure 3d, where $\alpha = 1, \beta = 1$). Figure 3b is for $\alpha = 10^{-3}$ and figure 3c for $\alpha = 10^{-1}$.

The even-parity cases are distinguished by the much longer lifetimes in the purely nonlinear cases (figure 4a; cf. figures 1 and 3). Figure 4 is for the fixed boundary case. The stabilization of the even-parity breather as α is changed from 10^{-3} (figure 4b) to 10^{-1} (figure 4c) and, finally 1 (figure 4d) is seen to be much more robust compared to the odd-parity cases. The periodic boundary case for the even-parity breather (figure 5) shows again the much reduced disruptions experienced in this case compared to the fixed boundary case. Breather in figure 5b, with $\alpha = 10^{-4}$ can be seen to be enjoying an enhanced lifetime compared to the purely nonlinear case in figure 5a. The breather of figure 5c, with $\alpha = 10^{-2}$ can be seen to be much more robust than the even-parity breather in the fixed boundary case with $\alpha = 10^{-1}$ (figure 4c).

The energy fluctuations in the long time limit as α is varied as above is shown in figure 6. These results are typical of how the system responds to changes in α, regardless of the parity of the breather and boundary conditions, and we chose the odd-parity breather in the fixed boundary case for this typical plot. The different case numbers refer to (Case 1) purely nonlinear case, (Case 2) $\alpha = 10^{-4}, \beta = 1$, (Case 3) $\alpha = 10^{-3}, \beta = 1$, (Case 4) $\alpha = 10^{-2}, \beta = 1$, (Case 5) $\alpha = 10^{-1}, \beta = 1$, (Case 6) $\alpha = 1, \beta = 1$. Finally, Case 7 corresponds to the purely linear case, i.e. $\alpha = 1, \beta = 0$. Figure 6a plots the time-averaged kinetic and potential energies in the long time limit. Note that the long time limit, when α has larger values, can still be carrying the breather while, for lower values of α, an equilibrium-like state would have resulted. We have carried out the time average over 300 time units at the end of the computational exercise. We have checked that these time

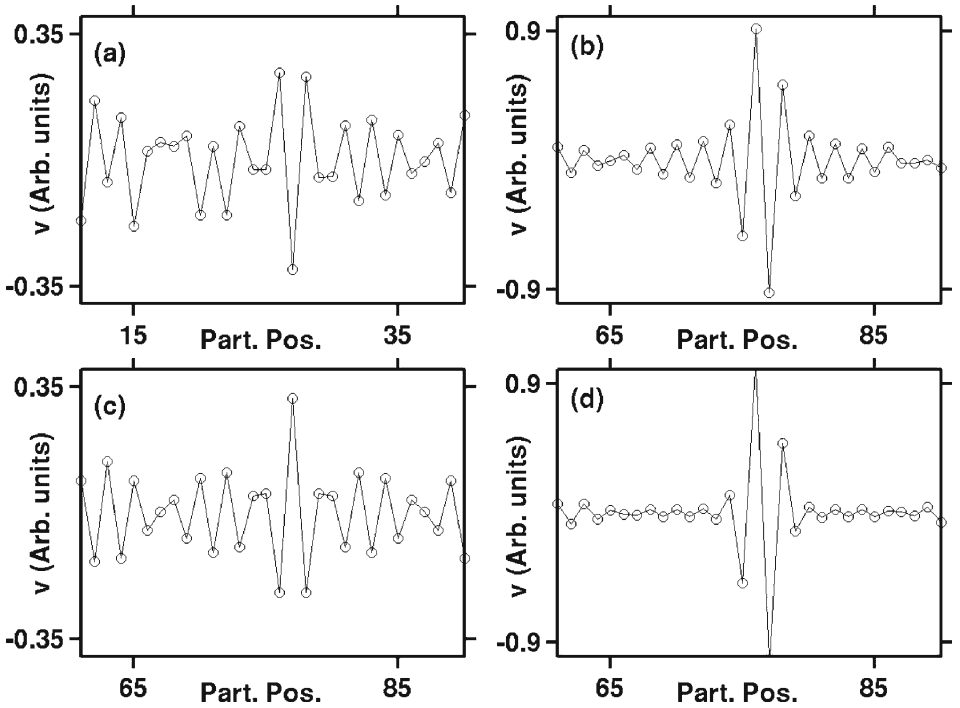

Figure 2. The velocity profile of the chain shown here confirms that the oscillation patterns of the odd- and even-parity cases are different. Figures 2a and 2b are for the fixed boundary case and figures 2c and 2d for the periodic boundary case. Figures 2a and 2c depict the odd-parity breathers and figures 2b and 2d the even-parity breathers.

averages are stationary by the end of the computational exercises. Figure 6b plots the standard deviations (SD) for those averages. This tells us about the level of fluctuations in the system. To bring out this feature in a better fashion, we plot in figure 6c the SD values as a percentage of the time average values. It is easily seen that the fluctuations are higher when α is comparable in strength to the β value. It is around 50% of the mean value when $\alpha = 10^{-1}$ and $\alpha = 1$ (Cases 5 and 6 respectively). These are the values when we obtain the longest lived breathers and thus it is the presence of the breathers which causes these large fluctuations in the time averages. In figure 6d, we have plotted on the y-axis the deviations of the time averages of kinetic and potential energies from $E/2$, the characteristic average value enjoyed equally by both kinetic and potential energies of the purely linear system. The deviation in the purely nonlinear state is seen to be maximum and the deviations smoothly reduce as α is increased. Note that the kinetic and potential energy values are equidistant from $E/2$.

4. Discussions and conclusions

Solitary and anti-solitary waves and breathers are objects of enormous interest in the study of nonlinear dynamical systems. The existence of these objects suggests that there may be

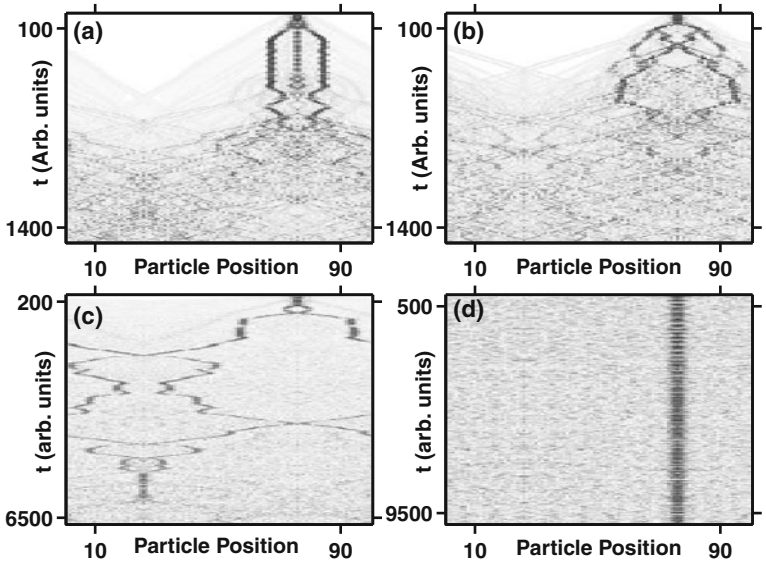

Figure 3. This figure is for the odd-parity breather in the periodic boundary case and should be compared with figure 1 which has fixed boundary conditions. It is seen that the breather of figure 3d is holding its position compared to the breather of figure 1d, even though both have identical parameter values of $\alpha = 1, \beta = 1$. For (**a**) $\alpha = 0$, (**b**) $\alpha = 10^{-3}$ and (**c**) $\alpha = 10^{-1}$, with all panels retaining $\beta = 1$.

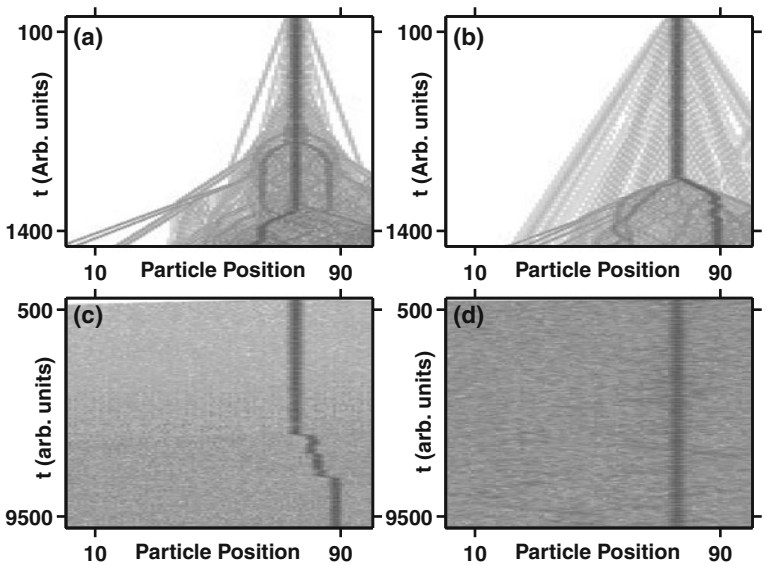

Figure 4. This figure is for the even-parity breather in the fixed boundary case and it is seen that the breather stabilizes further with small increments in α. The parameter values are $\beta = 1$ in all the panels and for (**a**) $\alpha = 0$, (**b**) $\alpha = 10^{-3}$, (**c**) $\alpha = 10^{-1}$ and (**d**) $\alpha = 1$.

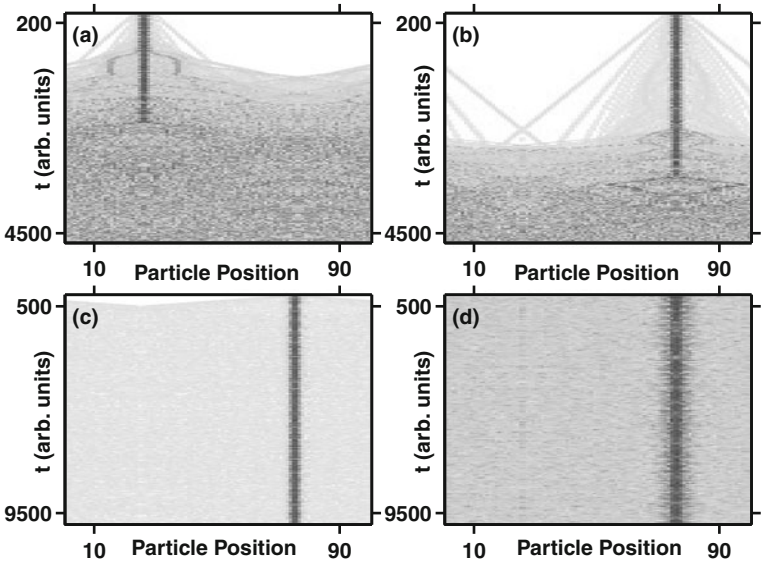

Figure 5. Even-parity breather in the periodic boundary case is shown here. The parameter values are $\beta = 1$ in all the panels and for (**a**) $\alpha = 0$, (**b**) $\alpha = 10^{-4}$, (**c**) $\alpha = 10^{-2}$ and (**d**) $\alpha = 1$.

novel possibilities in energy transport and capture using nonlinear lattices. In this work, we have focussed on DBs in pristine nonlinear chains. We have shown that the interplay of the harmonic and nonlinear pieces of the interparticle potential plays a crucial role in determining the lifetime (hence stability) of DBs. Below, we summarize this study in the broader context of the work we are pursuing.

In previous works [36–38], we studied the long time limit of these chains when a velocity perturbation was introduced at $t = 0$. Specifically, we looked at the purely nonlinear case with $\alpha = 0$. All the particles were at rest initially. A single particle was perturbed by imparting a finite velocity at $t = 0$. This perturbation led to the formation of solitary waves and anti-solitary waves, which subsequently interacted with each other and the boundaries. The eventual outcome of such interactions between the solitary, anti-solitary waves and the boundaries was the emergence of what we called a quasiequilibrium phase. This 'final state' had more significant energy fluctuations than the state with equipartitioned energy that would have emerged for the case of a purely harmonic chain. Upon turning on the linearity by letting $\alpha \neq 0$, we noticed that the solitary waves became unstable and a complex interplay of the solitary, anti-solitary and acoustic waves emerged.

If, instead of a velocity perturbation, we introduce a displacement perturbation in these lattices [46], we found that sustained and localized excitations, or DBs, emerged. The stability of these breathers turns out to depend strongly on the relative strengths of α and β.

In this work, we have treated the linearity as a perturbation to the nonlinearity. We have increased α from 0 (pure nonlinear system) to 1 in increments and investigated the stability aspect of the breathers. We found that the breathers became more stable when

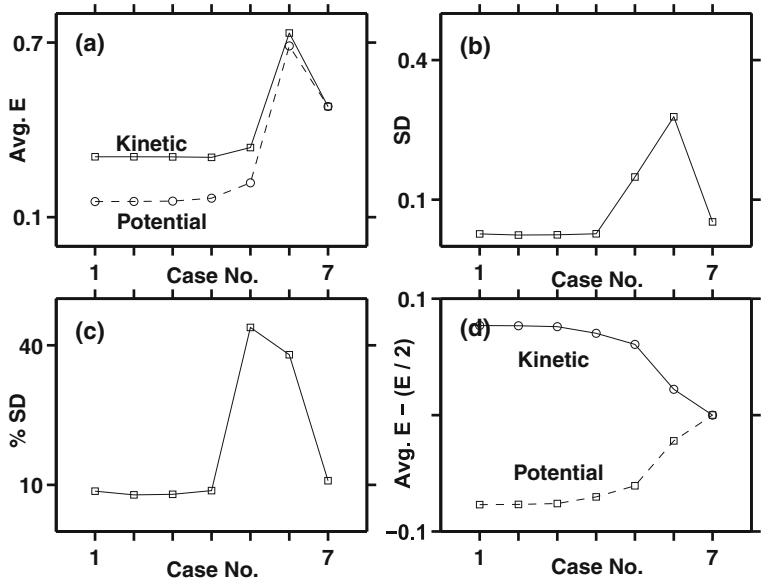

Figure 6. This figure is typical regardless of the parity of the breather and boundary conditions and is shown here using the odd-parity breather case with fixed boundaries. The different case indices from 1 to 7 refer, respectively, to the different cases corresponding to the parameter values with $\alpha = 0, \beta = 1$ (purely nonlinear state), $(\alpha = 10^{-4}, \beta = 1)$, $(\alpha = 10^{-3}, \beta = 1)$, $(\alpha = 10^{-2}, \beta = 1)$, $(\alpha = 10^{-1}, \beta = 1)$, $(\alpha = 1, \beta = 1)$ and $\alpha = 1, \beta = 0$ (purely linear state). In (**a**) the time-averaged kinetic and potential energies of the system in a long time limit is plotted. In (**b**), the standard deviation (SD) corresponding to the respective time averages is plotted. In (**c**) the SD as percentage of the corresponding time averages is plotted. In (**d**), the deviations of the time averages from $E/2$, the time averaged kinetic (potential) energy of the purely linear state with $\alpha = 1, \beta = 0$ is plotted.

$\alpha = \beta = 1$. We have increased α further, to values $\gg\beta$ and observed (not shown here) that the dynamics in those cases approximated the pure linear system with $\alpha = 1, \beta = 0$.

Displacement perturbations (all energy is potential in the beginning) lead to two different entities. If a single particle is displaced and the system was started from rest, we observed the formation of an odd-parity breather. If two particles were displaced away from each other and the system was started from rest, we observed the formation of an even-parity breather. In the purely nonlinear system, the odd-parity breather was less stable than the even-parity breather and split into three branches quite early in its evolution. However, in the presence of the linear term, we found that the odd-parity breather attained stability comparable to that of the even-parity breathers. In addition, the odd-parity breathers looked similar to the even-parity breathers in the energy–density plots. The particle motion we observed in the chain indicated that the odd- and even-parity breathers continue to show different oscillatory patterns. Some features of the differences in stability properties in the case of the odd- and even-parity breathers have been obtained analytically too and the reader is referred to Flach and Gorbach [44] and the references contained therein for the same.

It would be interesting to see what exactly causes the increased stabilization of the breathers when the harmonic term is switched on. In the purely nonlinear case, the leakage of energy from the breathers through the solitary and anti-solitary waves was a slow process and this gave the breathers their long lifetimes. In the presence of the acoustic waves, no energy leakage from the breather occurs due to a non-resonance condition [39,47]. However, solitary and anti-solitary waves still exist even in these systems though they are unstable in the presence of acoustic waves. So, energy leakage from the breathers presumably still occurs, albeit in a much reduced fashion, which probably is what leads to even longer lifetimes for the breathers. It is also conceivable that the nodes and anti-nodes associated with the acoustic oscillations contribute to increasing the stability of the breathers by providing good 'parking spots'. More studies are required to fully elucidate the complex interplay between these dynamical entities.

Acknowledgments

The authors acknowledge the support of the US Army Research Office.

References

[1] E Fermi, J Pasta and S Ulam, Los Alamos National Lab. Rept. LA-1940 (1955), reprinted in D C Mattis, *The many body problem* (World Scientific, Singapore, 1993) p. 851
[2] N J Zabusky and M D Kruskal, *Phys. Rev. Lett.* **15**, 240 (1965)
[3] For a review, see J Ford, *Phys. Rep.* **213**, 272 (1992)
[4] A S Dolgov, *Sov. Phys. Solid State* **28**, 907 (1986)
[5] A J Sievers and S Takeno, *Phys. Rev. Lett.* **61**, 970 (1986)
[6] R Dusi, G Vilani and M Wagner, *Phys. Rev.* **B54**, 9809 (1996)
[7] R Bourbonnais and R Maynard, *Phys. Rev. Lett*. **64**, 1397 (1990)
[8] V M Burlakov, S A Kiselev and V N Pyrkov, *Solid State Commun.* **74**, 327 (1990)
[9] S Takeno, K Kisoda and A J Sievers, *Prog. Theor. Phys. Suppl.* **94**, 242 (1988)
[10] J B Page, *Phys. Rev*. **B41**, 7835 (1996)
[11] K Yoshimura and S Watanabe, *J. Phys. Soc. Jpn* **60**, 82 (1991)
[12] S R Bickham and A J Sievers, *Phys. Rev*. **B43**, 2339 (1991)
[13] S Flach and C R Willis, *Phys. Rev. Lett.* **72**, 1777 (1994)
[14] R Dusi and M Wagner, *Phys. Rev*. **B51**, 15847 (1995)
[15] V F Nesterenko, *J. Appl. Mech. Tech. Phys.* **24**, 733 (1983)
[16] A N Lazaridi and V F Nesterenko, *J. Appl. Mech. Tech. Phys.* **26**, 405 (1985)
[17] V F Nesterenko, A N Lazaridi and E B Sibiryakov, *J. Appl. Mech. Tech. Phys.* **36**, 166 (1995)
[18] V F Nesterenko, *Dynamics of heterogeneous materials* (Springer, New York, 2001) Ch. 1
[19] S Sen, J Hong, J Bang, E Avalos and R Doney, *Phys. Rep.* **462**, 21 (2008)
[20] R S Sinkovits and S Sen, *Phys. Rev. Lett.* **74**, 2686 (1995)
[21] S Sen and R S Sinkovits, *Phys. Rev*. **E54**, 6857 (1996)
[22] C Coste, E Falcon and S Fauve, *Phys. Rev*. **E56**, 6104 (1997)
[23] G Friesecke and J A D Wattis, *Commun. Math. Phys.* **161**, 391 (1994)
[24] R S MacKay, *Phys. Lett.* **A251**, 191 (1999)
[25] J Y Ji and J Hong, *Phys. Lett.* **A260**, 60 (1999)
[26] S Sen, M Manciu and J D Wright, *Phys. Rev*. **E57**, 2386 (1998)
[27] A Chatterjee, *Phys. Rev*. **E59**, 5912 (1999)
[28] S Sen and M Manciu, *Physica* **A268**, 644 (1999)

[29] S Sen and M Manciu, *Phys. Rev.* **E64**, 056605 (2001)
[30] S Job, F Melo, A Sokolow and S Sen, *Phys. Rev. Lett.* **94**, 178002 (2005)
[31] M Manciu, S Sen and A J Hurd, *Phys. Rev.* **E63**, 016614 (2001)
[32] F Manciu and S Sen, *Phys. Rev.* **E66**, 016616 (2002)
[33] J Lee, S Park and I Yu, *Phys. Rev.* **E67**, 077707 (2003)
[34] Z Y Wen, S-J Wang, X-M Zhang and L Li, *Chin. Phys. Lett.* **24**, 2887 (2007)
[35] S Sen, T R Krishna Mohan and J M M Pfannes, *Physica* **A342**, 336 (2004)
[36] T R Krishna Mohan and S Sen, *Pramana – J. Phys.* **64**, 423 (2005)
[37] S Sen, J M M Pfannes and T R Krishna Mohan, *J. Korean Phys. Soc.* **46**, 57 (2005)
[38] E Avalos, R Doney and S Sen, *Chin. J. Phys.* **45**, 666 (2007)
[39] S Flach and A V Gorbach, *Phys. Rep.* **467**, 1 (2008)
[40] R Reigada, A Sarmiento and K Lindenberg, *Phys. Rev.* **E64**, 066608 (2001); *Chaos* **13**, 646 (2003)
[41] See D K Campbell, S Flach and Y S Kivshar, *Phys. Today* **57**, 43 (2004) for a recent review
[42] K W Sandusky, J B Page and K E Schmidt, *Phys. Rev.* **B46**, 6161 (1992)
[43] K W Sandusky and J B Page, *Phys. Rev.* **B50**, 866 (1994)
[44] S Flach and A V Gorbach, *Chaos* **15**, 015112 (2005)
[45] L Verlet, *Phys. Rev.* **159**, 98 (1967); *ibid.* **165**, 20 (1967)
M P Allen and D J Tildesley, *Computer simulation of liquids* (Clarendon, Oxford, 1987)
[46] Surajit Sen and T R Krishna Mohan, *Phys. Rev.* **E79**, 036603 (2009)
[47] S Flach, *Phys. Rev.* **E50**, 3134 (1994)